Crystallization of Rare Earth Oxide-Filled Polypropylene

JINGJIANG LIU, GONGBEN TANG, GUIJIE QU, HUARONG ZHOU, and QIPENG GUO*

Changchun Institute of Applied Chemistry, Academia Sinica, Changchun 130022, People's Republic of China

SYNOPSIS

A study has been made of the crystallization behavior of polypropylene (PP) filled with rare earth oxides under isothermal conditions. These rare earth oxides include lanthanum oxide (La_2O_3), yttrium oxide (Y_2O_3), and a mixture of rare earth oxides containing 70% Y_2O_3 (Y_2O_3–0.70). A differential scanning calorimeter was used to monitor the energetics of the crystallization process from the melt. During isothermal crystallization, dependence of the relative degree of crystallinity on time was described by the Avrami equation. It has been shown that the addition of any of the three rare earth oxides causes a considerable increase in the overall crystallization rate of PP but does not influence the mechanism of nucleation and growth of the PP crystals. The analysis of kinetic data according to nucleation theories shows that the increase in crystallization rate of PP in the composites is due to the decrease in surface energy of the extremity surfaces. The relative contents of the β-form in the composites are somewhat higher than that in the plain PP. However, the contents of the β-form in the plain PP and the composites are all very low relative to those of the α-form and the influence of the formation of the β-form on the crystallization kinetics can be neglected. © 1993 John Wiley & Sons, Inc.

INTRODUCTION

Polypropylene (PP) is one of the world's major plastics. Many studies have been done toward improving its performance by blending with other polymers or inorganic fillers. The original purpose of adding inorganic fillers to polymers was primarily one of cost reduction. However, in recent years, fillers increasingly have come to play a functional role, such as improving the stiffness or surface finish of a polymer. An inorganic filler can change the characteristics of a polymer in two ways: First, the properties of particles themselves such as size, shape, and modulus can have a profound effect, especially upon mechanical properties. Second, the particles may cause a change in the micromorphology of the polymer, which may then give rise to differences in observed bulk properties. For example, the surface of the filler may act as a nucleator for semicrystalline polymer and may thereby alter the amount or type of crystallinity. The minerals used as fillers in polypropylene (PP) are principally talc and calcium carbonate and, to a lesser extent, mica and wollastonite.[1-7] However, little attention has been paid to rare earth compounds used as fillers in polymers. As rare earth minerals are abundant in China, investigation of PP composites containing rare earth compounds is of practical significance.

In this paper, we present some results of our investigation on rare earth oxide-filled PP. These rare earth oxides include lanthanum oxide (La_2O_3), yttrium oxide (Y_2O_3), and a mixture of rare earth oxides containing 70% Y_2O_3 (Y_2O_3–0.70). Since these fillers can act as nucleators of PP and, hence, affect its crystallization behavior, which eventually determines the mechanical properties and processing behavior of the related composites, our attention was paid to the crystallization behavior of the filled PP and the influence of these rare earth oxides on the crystallization of PP.

EXPERIMENTAL

The sample of PP, PP1300, was commercially obtained from Yanshan Petrochemical Co., Beijing,

* To whom correspondence should be addressed.

Journal of Applied Polymer Science, Vol. 47, 2111-2116 (1993)
 CCC 0021-8995/93/122111-06

China. It had a melt index of 1.2 g/10 min (ASTM D1238) and a density of 0.91 g/cm^3 at 25°C. The rare earth oxides used were La_2O_3, Y_2O_3, and a mixture containing 70 wt% Y_2O_3 and other rare earth oxides. They were prepared in this laboratory and the characteristics of them are listed in Table I.

The composites of PP and rare earth oxides were prepared by a Brabender at 180°C. The plain PP1300 was subjected to the same procedure as were the composites in the Brabender at 180°C. The composites studied are presented in Table II.

A Perkin-Elmer DSC-2C differential scanning calorimeter (DSC) was employed to detect thermal transitions and to monitor the rate of heat flow from the sample during isothermal crystallization from the melt. The instrument was calibrated with an indium standard and the measurements were conducted under a nitrogen atmosphere. The sample weight used in the DSC cell was kept in the 8–12 mg range. The samples were first heated to 220°C at a rate of 80°C/min and maintained at this temperature for 10 min in order to remove prior thermal histories. They were then cooled to the appropriate crystallization temperature, T_c, at a rate of 80°C/min. The heat generated during the development of the crystalline phase was recorded up to a vanishing thermal effect and analyzed according to the usual procedure to obtain the relative degree of crystallinity, $\alpha(t)$:

$$\alpha(t) = X(t)/X(\infty) = \frac{\int_{t_0}^{t} (dH/dt)\, dt}{\int_{t_0}^{\infty} (\mathrm{dH}/dt)\, dt} \quad (1)$$

where t_0 is the time at which the sample attains isothermal conditions, as indicated by a flat base line after the initial spike in the thermal curve.

Absolute degree of crystallinity of PP in its pure state and in the composites was evaluated from the heat evolved during crystallization by means of the relationship

Table I Characteristics of the Rare Earth Oxides Used

Compound	Purity (%)	Average Particle Size (μm)
La_2O_3	99	0.05
Y_2O_3	99	0.02
Y_2O_3–0.70	70	0.05

Table II Samples of Composites Studied

Code	Filler	PP1300/Filler (w/w)
PP		100/0
PP–La	La_2O_3	100/0.5
PP–Y	Y_2O_3	100/0.5
PP–M	Y_2O_3–0.70	100/0.5

$$X(t) = \frac{\int_{t_0}^{t} (dH/dt)\, dt}{(1-\phi)\Delta H_f^0} \quad (2)$$

where $\Delta H_f^0 = 150$ J/g is the heat of fusion for 100% crystalline PP[8,9] and ϕ is the weight fraction of the filler in the composite.

To observe the melting behavior, some of the isothermally crystallized samples were reheated to 200°C at a rate of 10°C/min. The heat of fusion was calculated from the melting peak area, and the maximum of the endotherm was taken as the melting temperature, T_m.

RESULTS AND DISCUSSION

Typical crystallization isotherms, obtained by plotting $\alpha(t)$ against time, t, are reported in Figure 1 for the pure PP and for the PP–La, PP–Y and PP–M composites. From these curves, the half-time of crystallization $t_{1/2}$, defined as the time required for half of the final crystallinity to be developed, was obtained. The values of $t_{1/2}$ are listed in Table III, together with the other characteristics of crystallization. It can be seen that the addition of any of the three rare earth oxides causes an increase in the overall crystallization rate of PP.

The crystallization temperatures used for study range from 125–135°C. For even lower temperatures, crystallization will occur during the quenching process. For even higher temperatures, the mechanism of both nucleation and growth of crystallization of PP will change since it has been shown that the regime II → III crystallization transition occurs near 137°C,[9-11] according to the Hoffman's theory of crystallization kinetics.

The overall kinetics of PP and its composites follows the Avrami equation[12-14]:

$$\log\{-\ln[1-\alpha(t)]\} = \log K + n \log t \quad (3)$$

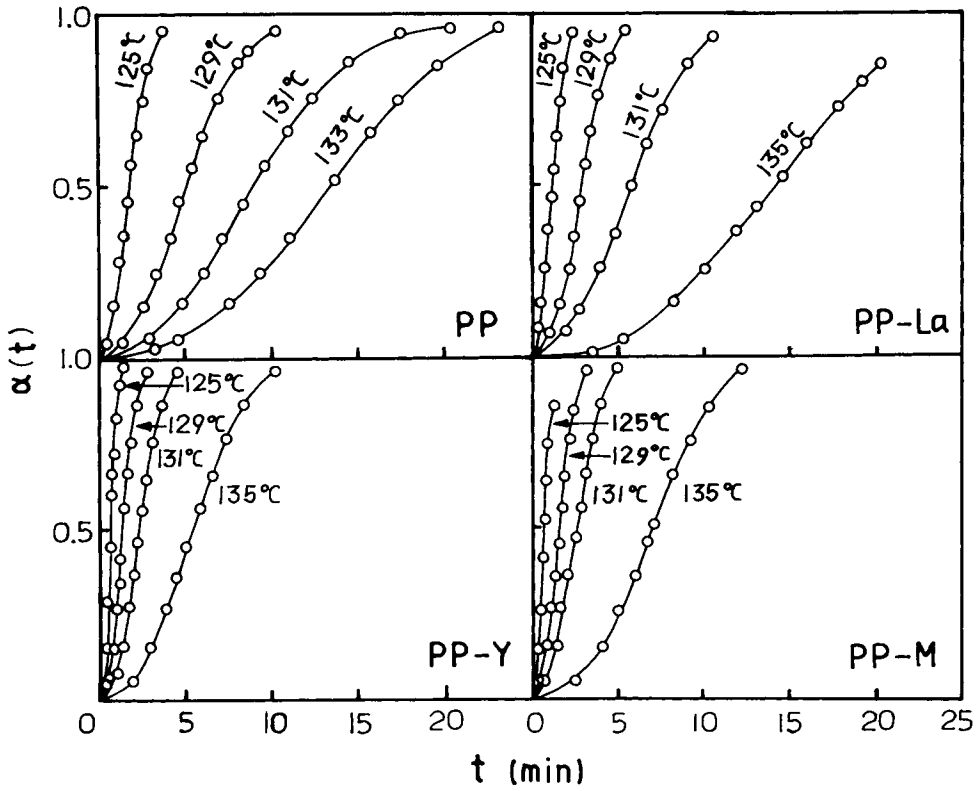

Figure 1 Development of relative degree of crystallinity with time for isothermal crystallization of PP and the composites.

where n, the Avrami index, and K, the kinetic rate constant, depend on the nucleation and growth mechanism of the crystals.[15]

Plots of $\log\{-\ln[1-\alpha(t)]\}$ against $\log t$ are linear, no change in the slope being observed until long times of conversion (Fig. 2). The experimental data

Table III Values of Various Crystallization Parameters of PP and the Composites

Sample	T_c (°C)	t_{max} (min)	$t_{1/2}$ (min)	ΔH_c (J/g)	$\alpha(t_{max})/\alpha(\infty)$ (%)
PP	133	13.7	13.5	104.9	52.0
	131	8.3	8.8	130.3	45.5
	129	4.7	5.0	110.6	46.0
	125	1.7	1.8	94.1	46.0
PP-La	135	13.9	13.7	96.4	51.3
	131	5.6	5.6	114.3	50.2
	129	2.8	2.9	97.2	46.4
	125	1.1	1.2	96.1	42.5
PP-Y	135	7.3	7.2	89.6	52.8
	131	2.6	2.6	89.9	50.0
	129	1.6	1.7	91.8	46.9
	125	0.6	0.6	89.7	44.0
PP-M	135	7.1	7.0	99.2	50.9
	131	2.4	2.5	97.5	47.0
	129	1.4	1.5	94.7	45.1
	125	0.5	0.6	102.3	39.0

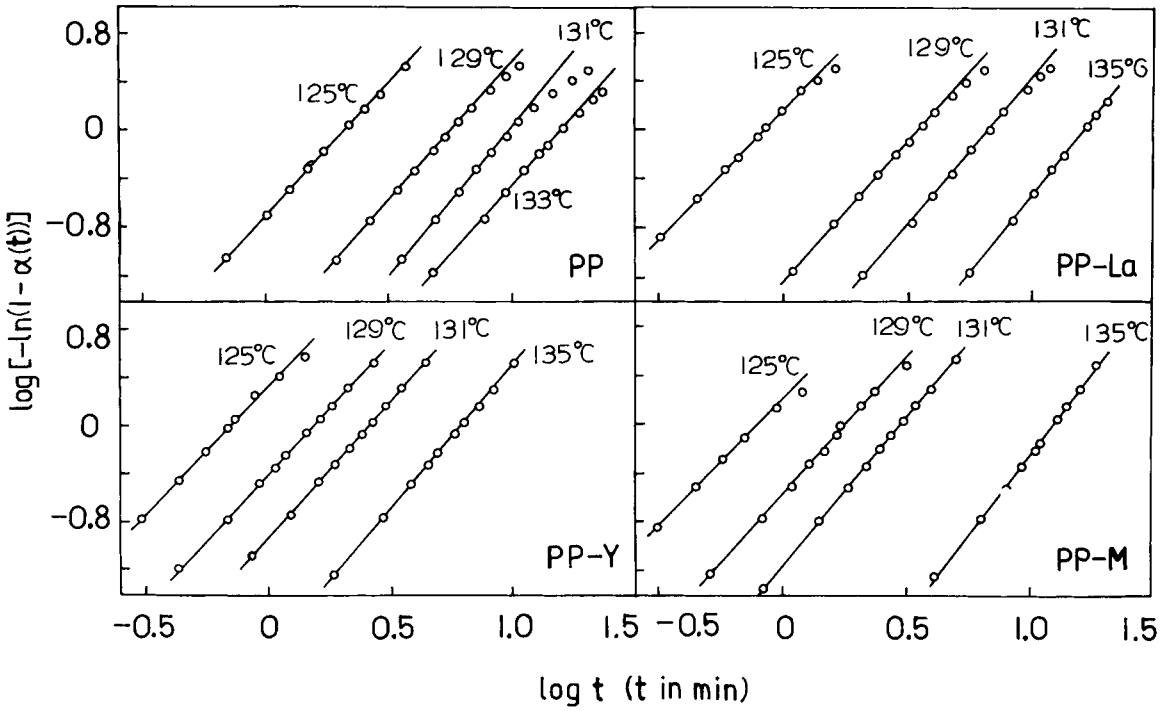

Figure 2 Plots of $\log\{-\ln[1-\alpha(t)]\}$ vs. $\log t$ for isothermal crystallization of PP and the composites.

appear to fit the Avrami equation well. The values of K and n determined by the intercepts and slopes, respectively, of these straight lines are given in Table IV.

The n values vary between 2.1 and 2.7 almost irrespective of T_c, whether the sample contains rare earth oxide or not, as well as type of the rare earth oxides. The fact that the Avrami index is almost

Table IV Values of Various Crystallization Parameters of PP and the Composites

Sample	T_c (°C)	n	K (S^{-n})	K_g (K^{-2})	σ_e (J/m^2)
PP	133	2.3	1.7×10^{-3}	1.22×10^6	0.203
	131	2.4	3.6×10^{-3}		
	129	2.3	1.9×10^{-2}		
	125	2.2	1.9×10^{-1}		
PP-La	135	2.7	5.9×10^{-4}	8.5×10^5	0.142
	131	2.4	1.1×10^{-2}		
	129	2.3	6.3×10^{-2}		
	125	2.1	5.1×10^{-1}		
PP-Y	135	2.7	3.2×10^{-3}	7.8×10^5	0.130
	131	2.5	7.0×10^{-2}		
	129	2.4	2.1×10^{-1}		
	125	2.3	1.7		
PP-M	135	2.6	4.5×10^{-3}	7.8×10^5	0.130
	131	2.4	7.1×10^{-2}		
	129	2.2	2.9×10^{-1}		
	125	2.3	1.7		

independent of whether the sample contains rare earth oxide or not and type of the rare earth oxides indicates that these rare earth oxides do not influence the mechanism of nucleation and growth of the PP crystal.

The kinetic theory of polymer crystallization developed by Hoffman and co-workers[16-18] has been generally used to analyze experimental data concerning spherulite growth rate. In this theory, the dependence of the growth rate G on the crystallization temperature T_c and on the undercooling $T = T_m^0 - T_c$ is described by the following equation:

$$G = G_0 \exp\left[-\frac{U^*}{R(T_c - T_\infty)}\right]\exp\left(-\frac{K_g}{fT_c\Delta T}\right) \quad (4)$$

where G_0 is a preexponential factor that is generally assumed to be constant or proportional to T_c; U^*, the activation energy for transport of polymer segments to the site of crystallization; R, the gas constant; and T_∞, a temperature somewhat below the glass transition temperature T_g; at this temperature, the viscosity is infinite. The quantity f is the correction factor for the heat of fusion; it takes into account the temperature dependence of ΔH_f^0. Usually, the following empirical expression is used for f:

$$f = \frac{2T_c}{T_m^0 + T_c} \quad (5)$$

K_g, the nucleation factor, is given by

$$K_g = \frac{Zb_0\sigma\sigma_e T_m^0}{k\Delta H_f^0} \quad (6)$$

where k is the Boltzmann's constant; b_0, the layer thickness; T_m^0, the equilibrium melting temperature; ΔH_f^0, the theoretical enthalpy of fusion per unit mass; σ and σ_e, the surface energies of the lateral and extremity surfaces, respectively; and Z, a coefficient that depends on the growth regime: $Z = 4$ in Regimes I and III, and $Z = 2$ in Regime II.[9-11]

It has been shown that it is possible to use calorimetric data obtained in isothermal conditions to discuss the overall crystallization behavior according to nucleation theories.[19] In fact, it can easily be shown that, under isokinetic conditions for the nucleation rate, N, and the linear growth rate, G, K is related to G by the simple relation

$$G = CK^{1/n} \quad (7)$$

where C is a constant. Combination of eqs. (4) and (7) can give

$$\ln C + \frac{1}{n}\ln K = \ln G_0 - \frac{U^*}{R(T_c - T_\infty)} - \frac{K_g}{fTc\Delta T} \quad (8)$$

The plots of $1/n \ln K + U^*/[R(T_c - T_\infty)]$ against $1/(fTc\Delta T)$ for the PP and its composites are shown in Figure 3. The experimental data fit the straight lines well. The slopes of the straight lines in the figure give the K_g values as listed in Table IV. By using eq. (6), these K_g values further give the values of σ_e for the PP and its composites, which is also shown in the last column of Table IV. In the analysis of our experimental results using eq. (8), we have employed the following[9,17]: $U^* = 6270$ J/mol, $T_m^0 = 481$ K, $\Delta H_f^0 = 150$ J/g, $\sigma = 8.79 \times 10^{-3}$ J/m^2, $b_0 = 0.656$ nm, and $T_\infty = T_g - 30°C$, with the experimental value $T_g = -10°C$. In our experiments, all the crystallization temperatures used are in Regime III; then, $Z = 4$.[9,17]

These results show that the addition of these rare earth oxides to the PP decreases the surface energy of the extremity surfaces and then considerably increases the crystallization rate of the PP; both Y_2O_3 and Y_2O_3–0.70 more efficiently increase the crystallization rate.

The melting behavior after the isothermal crystallization at 125°C for the PP and its composites is shown in Figure 4. It can be seen that all the samples exhibit two melting endothermic peaks,

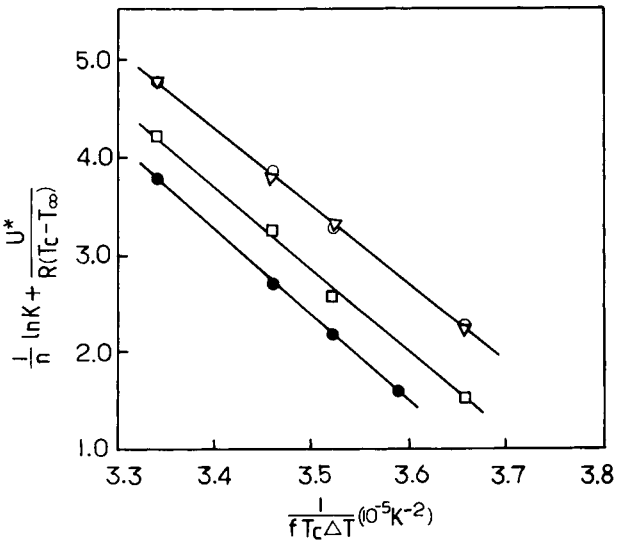

Figure 3 Plots of $1/n \ln K + U^*/[R(T_c - T_\infty)]$ against $1/(fT_c\Delta T)$ for (●) PP, (□) PP–La, (▽) PP–Y, and (○) PP–M.

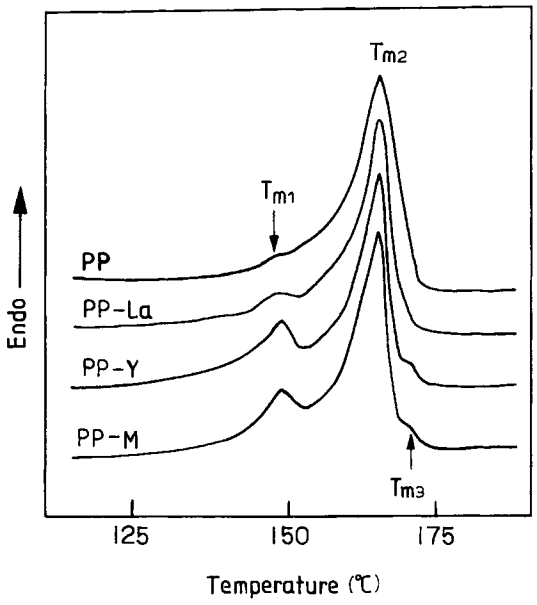

Figure 4 DSC scanning curves of PP and the composites after isothermal crystallization from the melt at 125°C. The heating rate is 10°C/min.

T_{m_1} = 149°C and T_{m_2} = 166°C, referred to the melting of the β- and α-forms of the PP crystallites, respectively. It is noted from the thermograms in Figure 4 that the relative contents of the β-form in the composites are all somewhat higher than that in the plain PP. However, the contents of the β-form in all the four samples are rather low relative to those of the α-form. This fact means that the influence of the formation of the β-form on the crystallization can be neglected. Figure 4 also shows that the samples PP–Y and PP–M exhibit another small melting peak T_{m_3} = 169°C, i.e., exhibit two melting peaks of the α-phase: T_{m_2} at 166°C and T_{m_3} at 169°C. It has been shown that the presence of two peaks of the α-phase was induced in some cases[20,21] by high temperature (> 155°C) conditioning; in other cases,[22–24] by appropriate choice of the temperature of crystallization (130°C < T_c < 150°C); and in still other cases, by the particular conditions under which the differential thermal analysis was performed: at a low scanning rate[25] (heating rate < 5°C/min) or on drawn samples restrained during the measurement.[24,26] In the present case, the splitting of the α-melting peak can be considered to be due to the recrystallization of the β-form to a stabler structure, α_2, and its melting during the heating. The same phenomenon has been observed and studied in detail in our previous work on the wollastonite-filled PP composites.[7]

REFERENCES

1. A. M. Riley, C. D. Paynter, P. M. MaGenity, and J. M. Adams, *Plast. Rubber Proc. Appl.*, **14**, 85 (1990).
2. G. E. Padawar and N. Beecher, *Polym. Eng. Sci.*, **10**, 185 (1970).
3. J. Menozel and J. Varga, *J. Therm. Anal.*, **28**, 161 (1983).
4. A. K. Gupta, K. R. Srinivasan, and P. K. Kumar, *J. Appl. Polym. Sci.*, **43**, 451 (1991).
5. J. E. Stamhuis, *Polym. Compos.*, **9**, 280 (1988).
6. M. G. Huson and W. J. McGill, *J. Polym. Sci. Polym. Chem. Ed.*, **22**, 3571 (1984).
7. J. Liu, X. Wei, and Q. Guo, *J. Appl. Polym. Sci.*, **41**, 2829 (1990).
8. B. Wunderlich, *Macromolecular Physics*, Academic Press, New York, 1980, Vol. 3.
9. B. Monasse and J. M. Haudin, *Colloid Polym. Sci.*, **263**, 822 (1985).
10. J. J. James, Z. D. C. Stephen, and A. G. Paul, *Macromolecules*, **24**, 2253 (1991).
11. E. J. Clark and J. D. Hoffman, *Macromolecules*, **17**, 878 (1984).
12. M. Avrami, *J. Chem. Phys.*, **7**, 1133 (1939).
13. M. Avrami, *J. Chem. Phys.*, **8**, 212 (1940).
14. M. Avrami, *J. Chem. Phys.*, **9**, 177 (1941).
15. J. M. Schultz, *Polymeric Materials Science*, Prentice-Hall, New York, 1981.
16. J. D. Hoffman, *Soc. Plast. Eng. Trans.*, **4**, 315 (1960).
17. J. D. Hoffman, L. J. Frolen, G. S. Ross, and J. I. Lauritzen, *J. Res. Natl. Bur. Stand. U.S.*, **79A**, 671 (1975).
18. J. D. Hoffman, *Polymer*, **24**, 3 (1983).
19. J. D. Hoffman, G. T. Davies, and J. L. Lauritzen, Jr., in *Treatise in Solid State Chemistry*, N. B. Hannay, Ed. Plenum Press, New York, 1976, Vol. 3, Chap. 7.
20. W. W. Cox and A. A. Duswalt, *Polym. Eng. Sci.*, **7**, 1 (1967).
21. K. D. Pae and J. A. Sauer, *J. Appl. Polym. Sci.*, **12**, 1901 (1968).
22. K. Kamide and K. Yamaguchi, *Makromol. Chem.*, **162**, 219 (1972).
23. C. L. Siegloff and K. J. O'Leary, *Polym. Prepr. Am. Chem. Soc. Div. Polym. Chem.*, **10**, 57 (1969).
24. R. J. Samuels, *J. Polym. Sci., Polym. Phys. Ed.*, **13**, 1417 (1975).
25. P. Jacoby, B. H. Bersted, W. J. Kissel, and C. E. Smith, *J. Polym. Sci. Polym. Phys. Ed.*, **24**, 461 (1986).
26. D. T. F. Pals, P. Van der Zee, and J. H. M. Albers, *J. Macromol Sci. Phys.*, **6**, 739 (1972).

Received February 11, 1992
Accepted May 26, 1992